GEM TN-93-280
MIT-GEM-EM-11

Electromagnetic Forces on Major Iron Components of the SSC GEM Detector

R.L. Myatt
Plasma Fusion Center, Massachusetts Institute of Technology

January 15, 1993

Abstract:

The GEM Detector includes many sizable carbon steel components, such as the flux shapers, central membrane, vacuum vessels, and associated supporting structures, all of which become magnetized in the presence of the coil's magnetic field. The objective of this report is to determine, by the finite element method, the electromagnetic forces on these iron components. This is achieved with two ANSYS models: a 3-D model which includes only the details of the flux shaper and associated support structure; and an axisymmetric model which includes the flux shaper and its supporting membranes, the coil and vacuum vessel, and the central membrane.

MIT-GEM-EM-11

Electromagnetic Forces on Major Iron Components of the SSC GEM Detector

January 15, 1992

R.L. Myatt

This document and all reports and memoranda in this series are intended as a record of work in progress. They are for use in informal discussions of design and fabrication alternatives. This material is subject to change and should not, therefore, be published or referred to in the open literature. Conclusions are preliminary and distribution should be strictly limited.

Plasma Fusion Center
Massachusetts Institute of Technology
Cambridge, MA 02139

MIT GEM DETECTOR Memoranda
Approval Sheet

B.A. Smith
Project Engineer

1/15/93
Date

R.D. Pillsbury, Jr.
Technical Manager

1/15/93
Date

A.M. Dawson
Technical Editor

15 Jan 93
Date

1.0 Introduction

The GEM Detector includes many sizable carbon steel components, such as the flux shapers, central membrane, vacuum vessels, and associated supporting structures, all of which become magnetized in the presence of the coil's magnetic field. The objective of this report is to determine, by the finite element method, the electromagnetic forces on these iron components. This is achieved with two ANSYS[1] models: a 3-D model which includes only the details of the flux shaper and associated support structure; and an axisymmetric model which includes the flux shaper and its supporting membranes, the coil and vacuum vessel, and the central membrane.

2.0 Conclusions

The 3-D analysis provides loads on the nonaxisymmetric flux shaper support members. **The forces presented act on the members explicitly included in the model. Symmetry applies to these results, and must be considered in determining the total load on the entire structural element.** For example, the -2.0 MN magnetic body force acting on the modeled Flux Shaper support members must be doubled to determine the total axial attraction it has to the other end of the detector. See the notes under the individual tables for further clarification.

The 2-D axisymmetric results are summarized in tables listing net body forces and figures showing traction force vectors for each of the major axisymmetric components in the GEM detector. The finite element mesh has been refined several times, and the effects of linear and quadratic elements has been studied. Also, two separate force calculation methods have been employed. The electromagnetic forces have converged to the values presented.

3.0 Analysis Methodology

3.1 3-D Flux Shaper Support Structure Model

A 3-D finite element model is developed to estimate the magnetic forces on the nonaxisymmetric iron members of the flux shaper support structure. Figure 3.1-1 shows the coils and the iron components of the model, which includes three large box sections and two flux shaper support membranes. The model also includes air elements which completely surround the iron elements and extend to an imposed far-field boundary. These air elements are excluded from the figure since they would obscure the details of the iron components and current source primitives. Figure 3.1-2 is included to detail the iron elements.

The analysis is based on the ANSYS Difference Scalar Potential (DSP) formulation, which solves the magnetic field equations with a single degree of freedom, MAG. The coils are

---

[1] *ANSYS, Rev. 4.4A for 3-D analyses, Rev. 5.0 Beta 3 for 2-D analyses, Swanson Analysis Systems, Inc., Houston, PA*

modeled as so-called source primitives, defined by their position in space, radial and axial builds, and current. The solution is nonlinear and iterative due to the saturation effects of the iron components.

The model is built with the ANSYS parametric design language which makes refinements of the finite element grid and changes in critical dimensions an easy task. Although the dimensions of the iron components remain unchanged throughout the analyses, significant work is done to quantify the effects of the mesh density.

The baseline B-H curve used in the program is shown in Table 3.1-1 and represents a reduced set of values from the widely used MAP B-H curve[2]. The code passes a cubic spline through the input data to ensure smooth interpolations and well-behaved convergence.

The geometry is assumed to be symmetric about a vertical midplane which separates the two-coil set (X-Y plane), thus allowing the first simplification to the model. The appropriate "flux-normal" boundary condition is imposed by setting the MAG degree of freedom to zero for all nodes on this Z=0 plane. A second symmetry condition occurs in the vertical-longitudinal (Y-Z) plane and provides another means of simplifying the model. Here, the flux density is parallel to the plane, which is the natural boundary condition in the scalar potential formulation (no specification on the MAG degree of freedom is required).

ANSYS' automated Virtual Displacement force calculation procedure is invoked to determine the forces acting on the iron elements included explicitly in the model.

3.2 2-D Axisymmetric Components Model

Other than the grossly asymmetric members of the flux shaper support geometry, the baseline detector is essentially axisymmetric. A detailed 2-D axisymmetric model is used to capture the forces on these axisymmetric iron components. A plot of the 2-D model is shown in Figure 3.2-1. As with the previous model, air is excluded from the plot to highlight the structural components of the geometry. This model focuses on the details of the flux shaper and support membrane, the vacuum vessel and the central membrane.

For this problem the program[3] uses a quadratic element to solve the 2-D vector potential magnetic field equations. In-plane fields (B_x and B_y) are produced by the out-of-plane potential, A_z. As before, the flux-normal symmetry condition exists at the Y=0 midplane but, in this formulation, it is the natural boundary condition and no restriction to A_z is required. A_z is set to zero along the axis of revolution (X=0) and at the far field boundaries, where a flux-parallel condition is required. This latest version of ANSYS allows the user to input up to 100 B-H data points. In this case, the full 36-point curve of Ref. 2 is used.

It should be noted that some effort has been put into verifying the accuracy of the force calculation. In addition to many mesh refinements, two force calculation methods have been

---

[2] *Robert D. Pillsbury, Jr., MAP User's Manual, PFC/RR-91-5, December 1991, MIT Plasma Fusion Center, Cambridge, MA 02139*

[3] *ANSYS 5.0, Beta 3, Swanson Analysis Systems Inc., Houston, PA*

employed; the Magnetic Virtual Displacement (MVDI) and Maxwell surface loading (MXWF). The results show reasonably good agreement between these methods. However, the MVDI loading method with the quadratic element formulation seems to produce the most consistent results, and remains the basis for the tabulated values presented here.

4.0 Results

4.1 Forces on Nonaxisymmetric Flux Shaper Supports

The net magnetic forces acting on the iron support structure of the model are summarized in Table 4.1-1. It is important to understand that these forces represent the loads on the elements explicitly included in the quarter model of the detector. It is also important to keep in mind the symmetry of the problem when applying these net loads in a structural analysis. Lateral (X) forces calculated for the quarter model are balanced by forces on the mirror image iron members (about the X=0 plane) resulting in a zero net load on the structure. For example, the table indicates that the box section support members, as a whole, experiences a net 2.1 MN X-directed magnetic force. By implication, the other half of the box section would experience a -2.1 MN X-directed magnetic force, which would essentially put the structure into compression by 2.1 MN. The symmetry works the opposite way for vertical (Y) and axial (Z) forces, which are additive to those of the other half of the geometry.

Continuing the example, the 1.8 MN vertical load represents half of the total vertical load acting on this group of support members. As a whole, these members will experience a 3.6 MN vertical load. The axial forces are dealt with in a similar way such that these members located in the $Z > 0$ space experiences a 4 MN attraction towards the other end of the detector.

4.2 Forces on Axisymmetric Detector Components

In the axisymmetric analysis, all major iron components are included in the model. The results are limited to net axial and radial forces as shown in Tables 4.2-1 and 4.2-2, respectively. To help illustrate the force distribution over the surface of the body, vector plots are included for each of the major components. Figure 4.2-1 shows the $\mathbf{I} \times \mathbf{B}$ body forces in the coil. Loads are proportional to the vector length (2.54 cm maximum) and have units of N/radian. Figure 4.2-2 shows the so-called traction forces acting on the flux shaper, which has a net axial load of -9.9 MN and net radial load of about 1.7 MN/radian. Figure 4.2-3 shows a similar plot of the traction forces acting on the vacuum vessel. To help clarify these results, Figures 4.2-3i and 4.2-3o are included to show the same information for elements inside and outside the winding inner radius (9.466 m), respectively. Figures 4.2-4 and 4.2-5 show similar results for the central and flux shaper support membranes, respectively.

Table 3.1-1 Ferromagnetic Behavior of Iron Material

Baseline B-H Curve	
B [T]	H [A/m]
0.89443	178.3
1.200	294
1.400	501
1.500	797
1.550	1153
1.600	1795
1.650	2862
1.750	6044
1.800	8122
1.850	10585
1.900	13608
2.000	21168
2.050	26754
2.100	33757
2.125	38217
2.175	52443
2.200	66002
2.250	99471
2.3443	169590
2.8498	566950

Notes:

1. The 3-D analysis of the flux shaper and support structure use this B-H curve, which is a subset of the data provided in Ref. 2.
2. The axisymmetric analysis uses the complete B-H curve of Ref. 2.

Table 4.1-1 Forces on the FS Box Section Support Members

Net Load on Box Section Support Members Included Explicitly in the FE Quarter Model		
Lateral (X)	Vertical (Y)	Axial (Z)
2.1 MN	1.8 MN	-2.0 MN

Note:

The finite element model employs quarter symmetry. Therefore, the results presented here represent one-half of the forces acting on one flux shaper support structure. For example, the net lateral (X) load on the support is zero. The net vertical (Y) load is 3.6 MN, and the net axial (Z) load is -4.0 MN.

Table 4.2-1 Axial Forces on Major Axisymmetric GEM Detector Iron Components

Component	Net Axial Electro-magnetic Force [MN]	Total of Positive & Negative Axial Forces [MN] (see note 2)
Coil	**(I x B)** -49.7	18.7/-68.4
Flux Shaper	-9.9	7.0/-16.9
Vacuum Vessel VV Inside R_c[1] VV Outside R_c[1]	0.9 0.8 0.1	82.6/-81.7 66.7/-65.9 15.8/-15.7
Central Membrane[3]	3.0	48.8/-45.8
Flux Shaper Membranes	-1.0	8.0/-9.0

Notes:

1. R_c is the inside radius of the winding (9.466 m).

2. The second column is included here to show the potential for error in some of the force calculations. For example, the net axial load on the inner half of the vacuum vessel is a small fraction of the total calculated load.

3. There is an equal and opposite axial load on the other half of the central membrane located in the negative Y.

Table 4.2-2 Radial Forces on Major Axisymmetric GEM Detector Iron Components

Component	Radial Electro-magnetic Force [MN/rad]
Coil	**(I x B)** 36.2
Flux Shaper	1.7
Vacuum Vessel VV Inside R_c[1] VV Outside R_c[1]	 -0.9 ~0
Central Membrane[3]	-0.1
Flux Shaper Membrane	0.2

Notes:

1. R_c is the inside radius of the winding (9.466 m).

2. Forces are on a per radian basis.

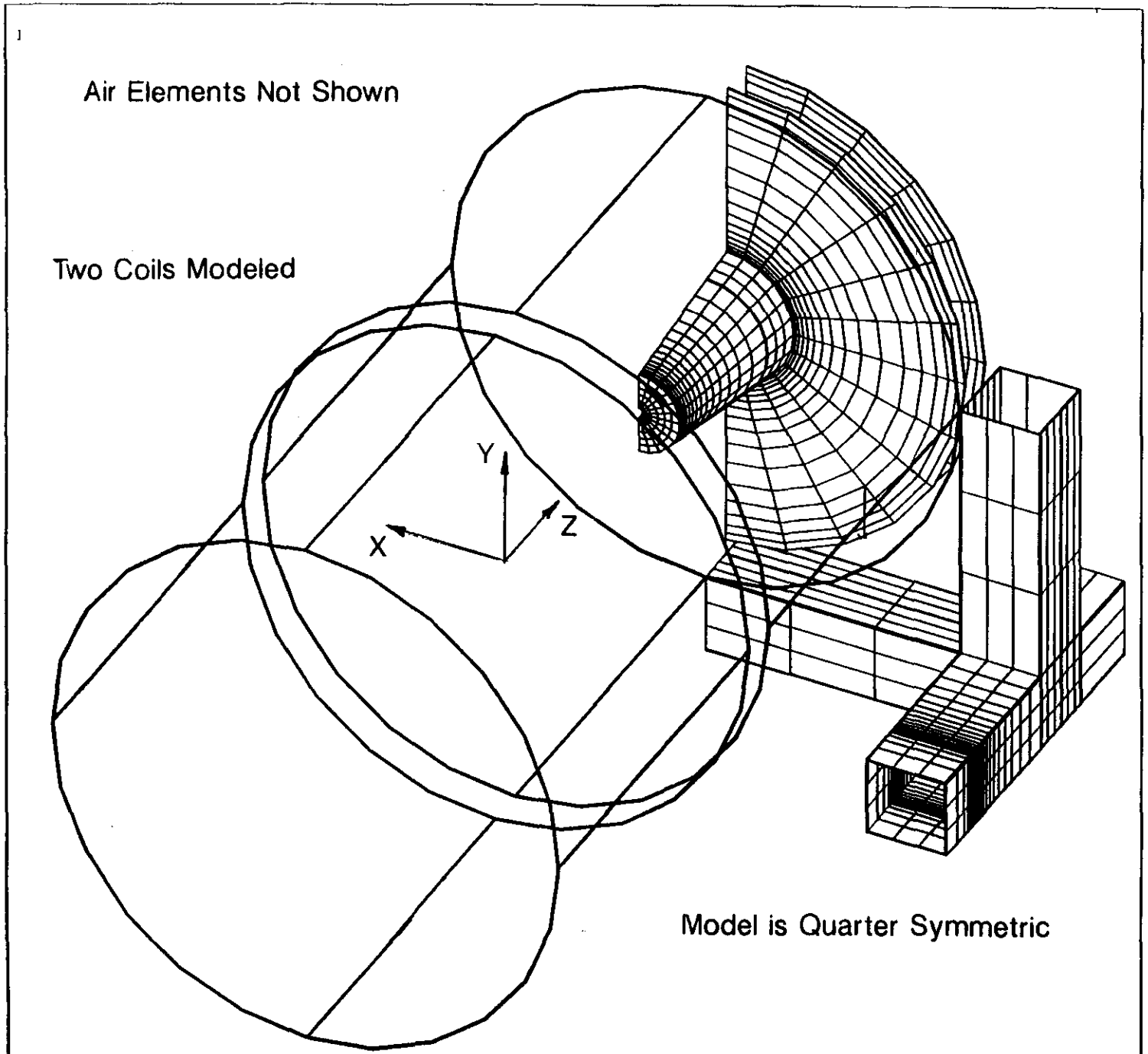

ANSYS 4.4A
DEC 30 1992
12:02:18
PLOT NO. 1
PREP7 ELEMENTS
MAT NUM
SOUR

XV =-1
YV =1.5
ZV =-2
*DIST=19
*XF =-2.5
PRECISE HIDDEN

Fig 3.1-1 Model of Flux Shaper, Support Members and Coil Primitives

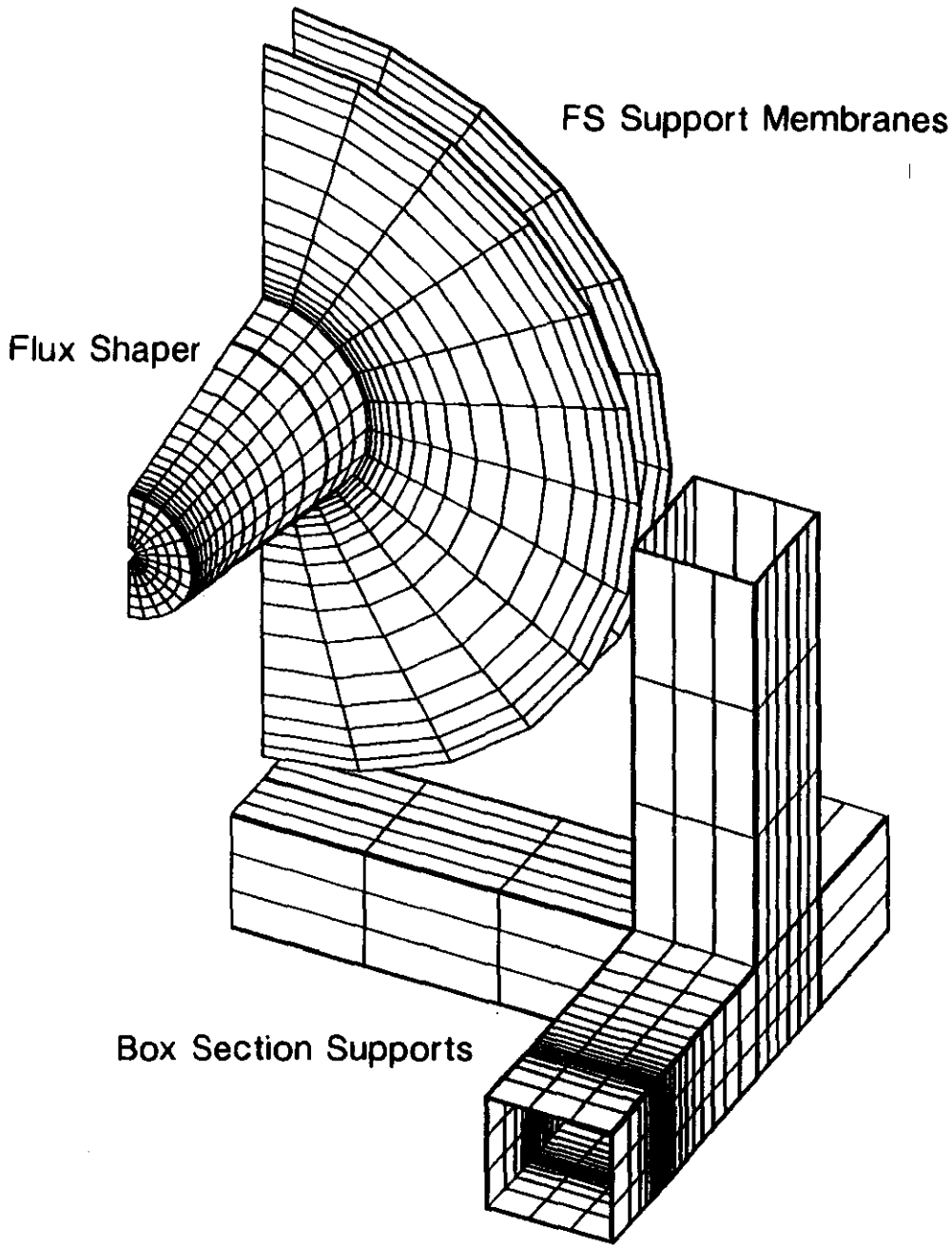

ANSYS 4.4A
DEC 30 1992
11:24:45
PLOT NO. 1
PREP7 ELEMENTS
MAT NUM

XV =-1
YV =1.5
ZV =-2
DIST=15.067
XF =-6.25
YF =-1.687
ZF =14.625
PRECISE HIDDEN

Fig 3.1-2 Iron Components

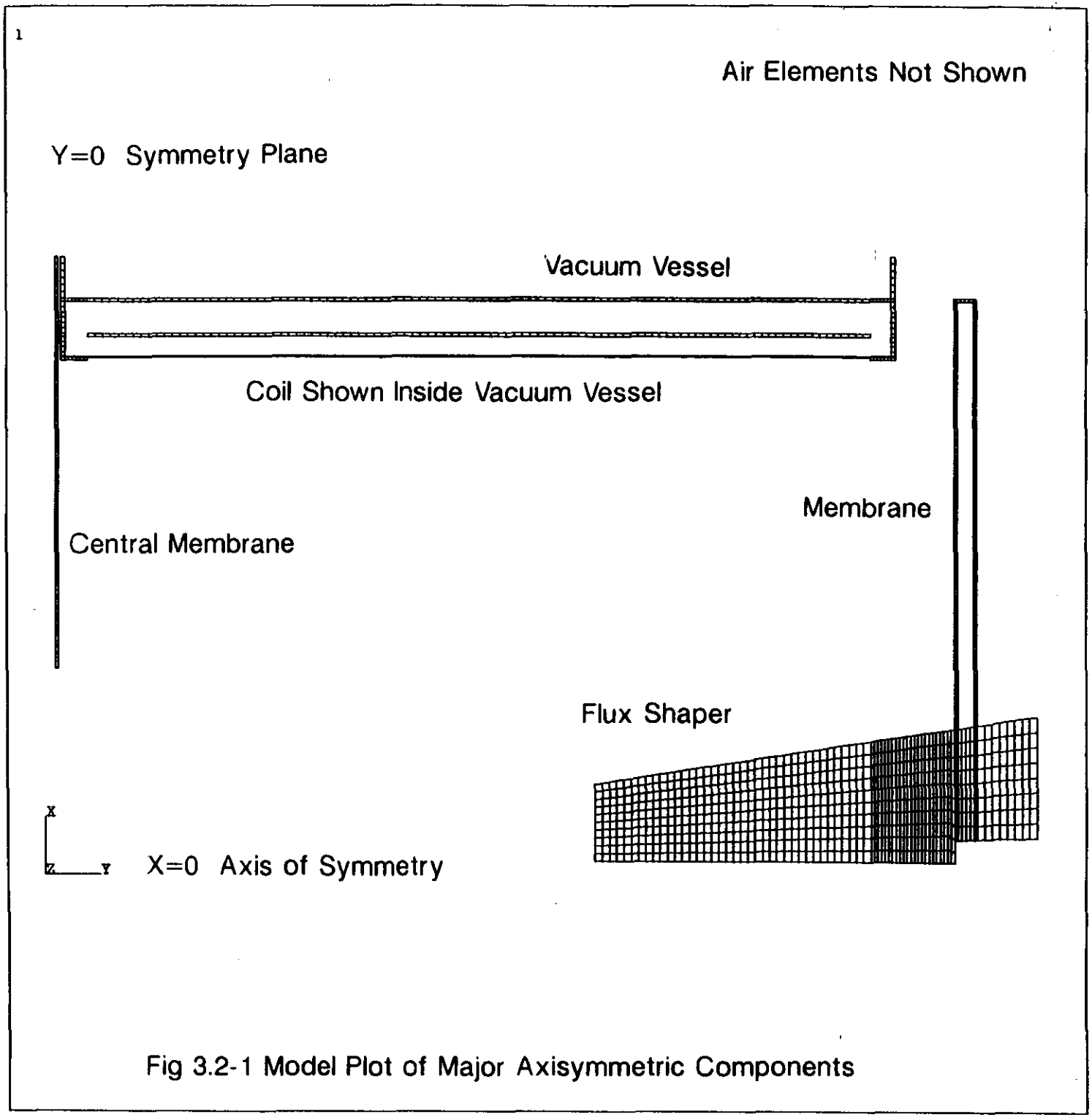

ANSYS 5.0
OCT 27 1992
09:24:02
PLOT NO. 1
ELEMENTS
MAT NUM

ZV =-1
DIST=9.79
XF =5.55
YF =9.1
VUP =X

Fig 3.2-1 Model Plot of Major Axisymmetric Components

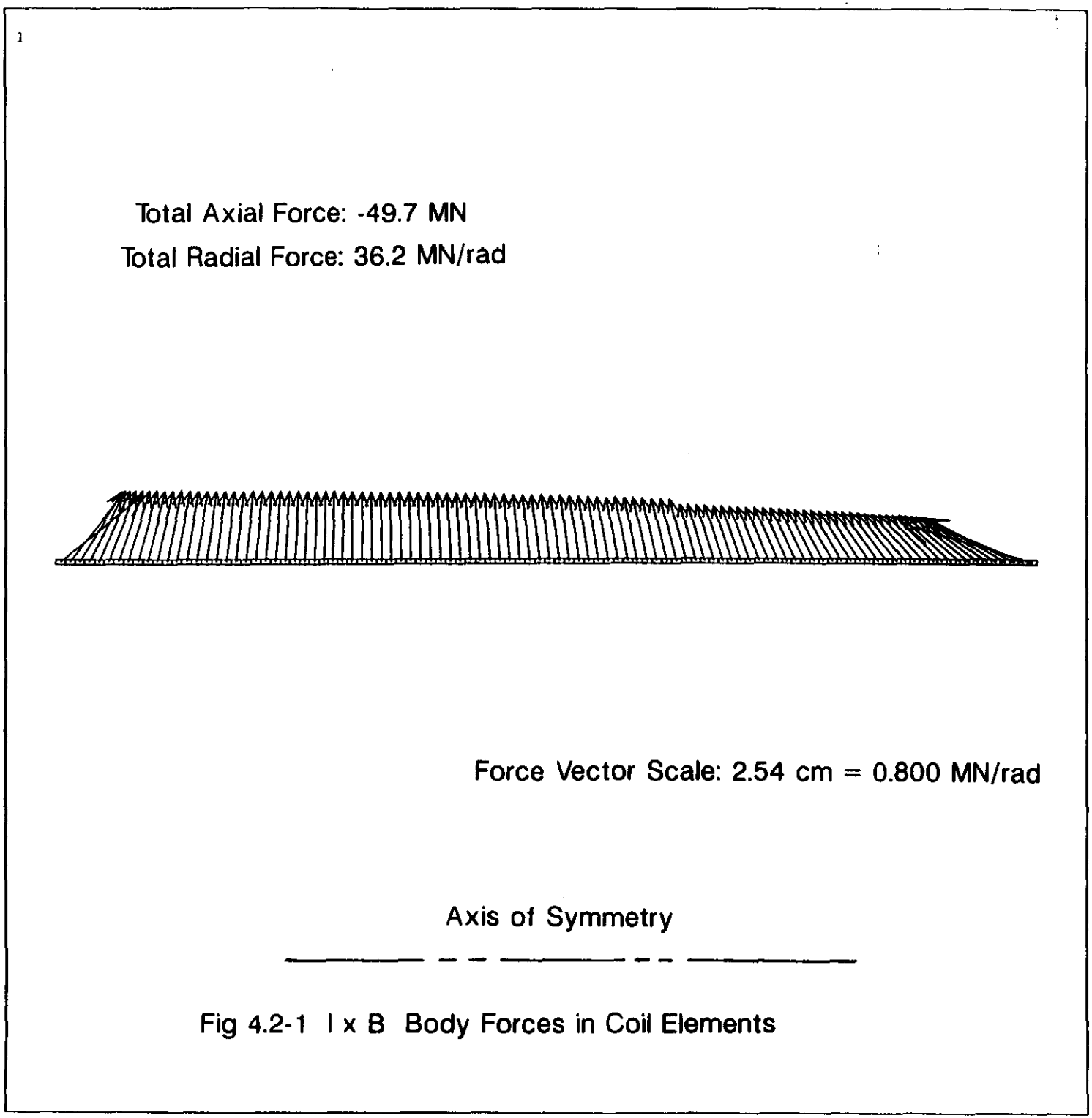

ANSYS 5.0
DEC 31 1992
12:57:48
PLOT NO. 2
VECTOR
STEP=2
SUB =1
TIME=2
FRAD
ELEM=8131
MIN=335218
MAX=800268
[N/rad]
335218
393349
451481
509612
567743
625874
684006
742137
800268

Fig 4.2-1 I x B Body Forces in Coil Elements

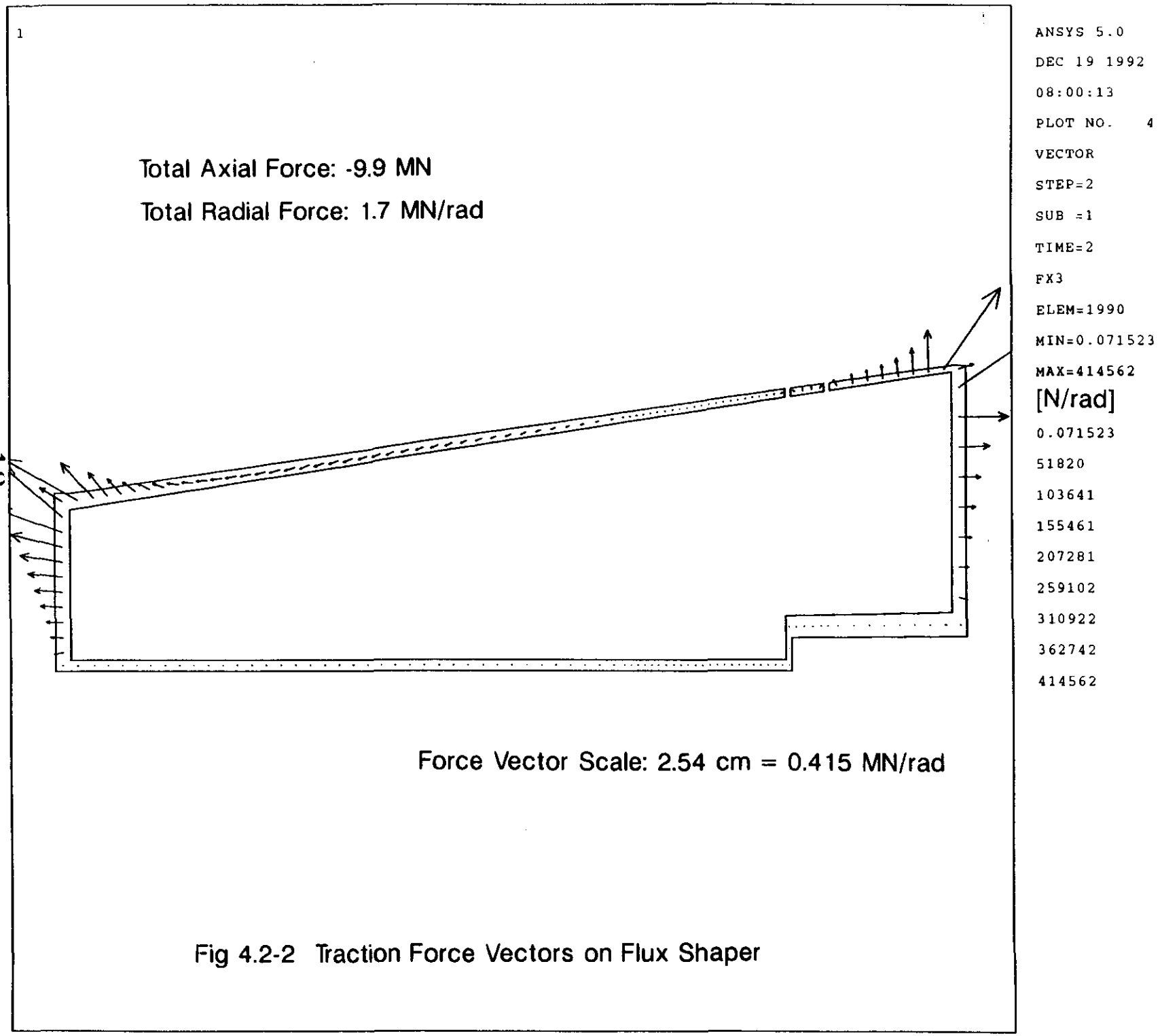

Fig 4.2-2 Traction Force Vectors on Flux Shaper

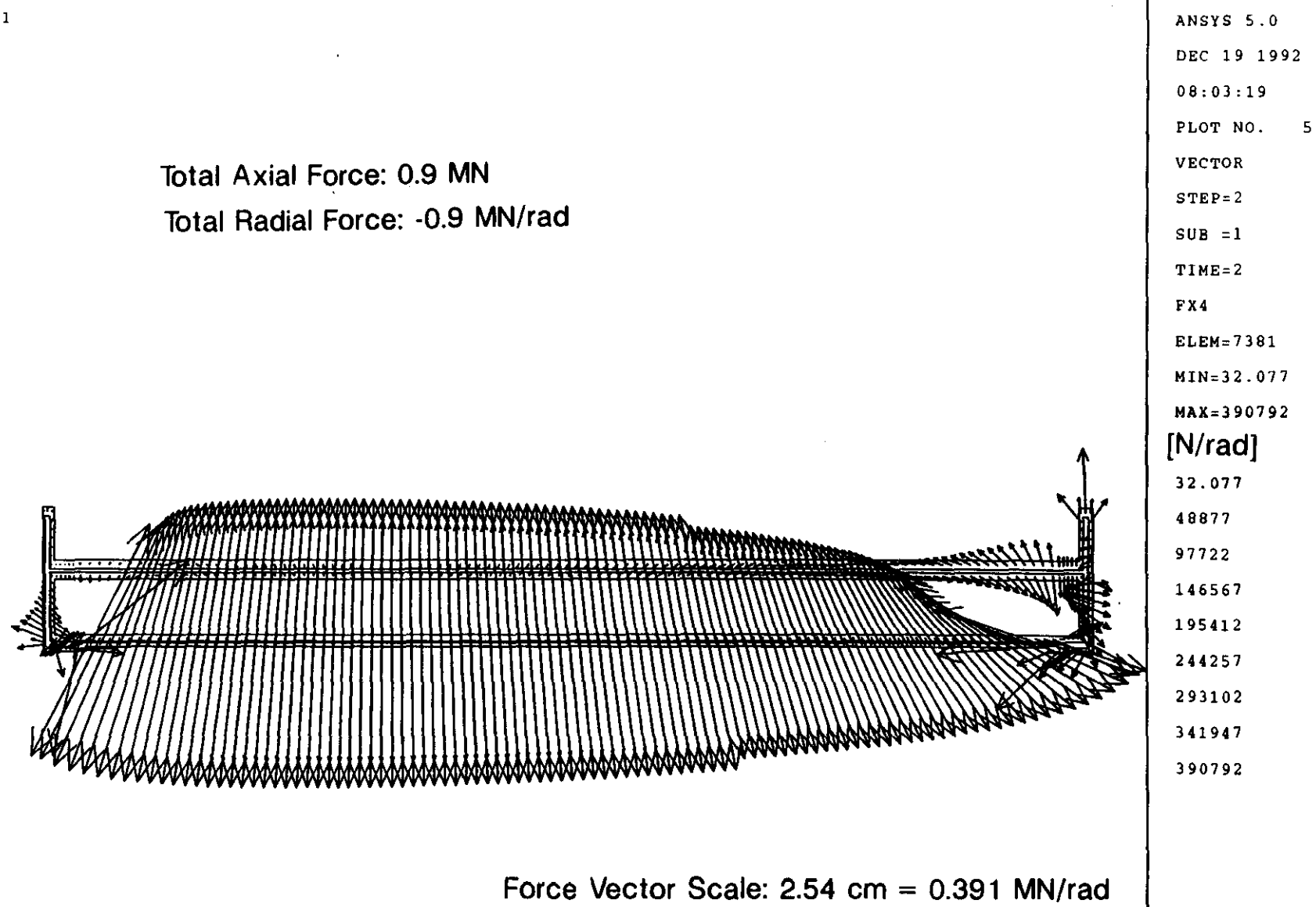

Fig 4.2-3 Traction Force Vectors on Vacuum Vessel

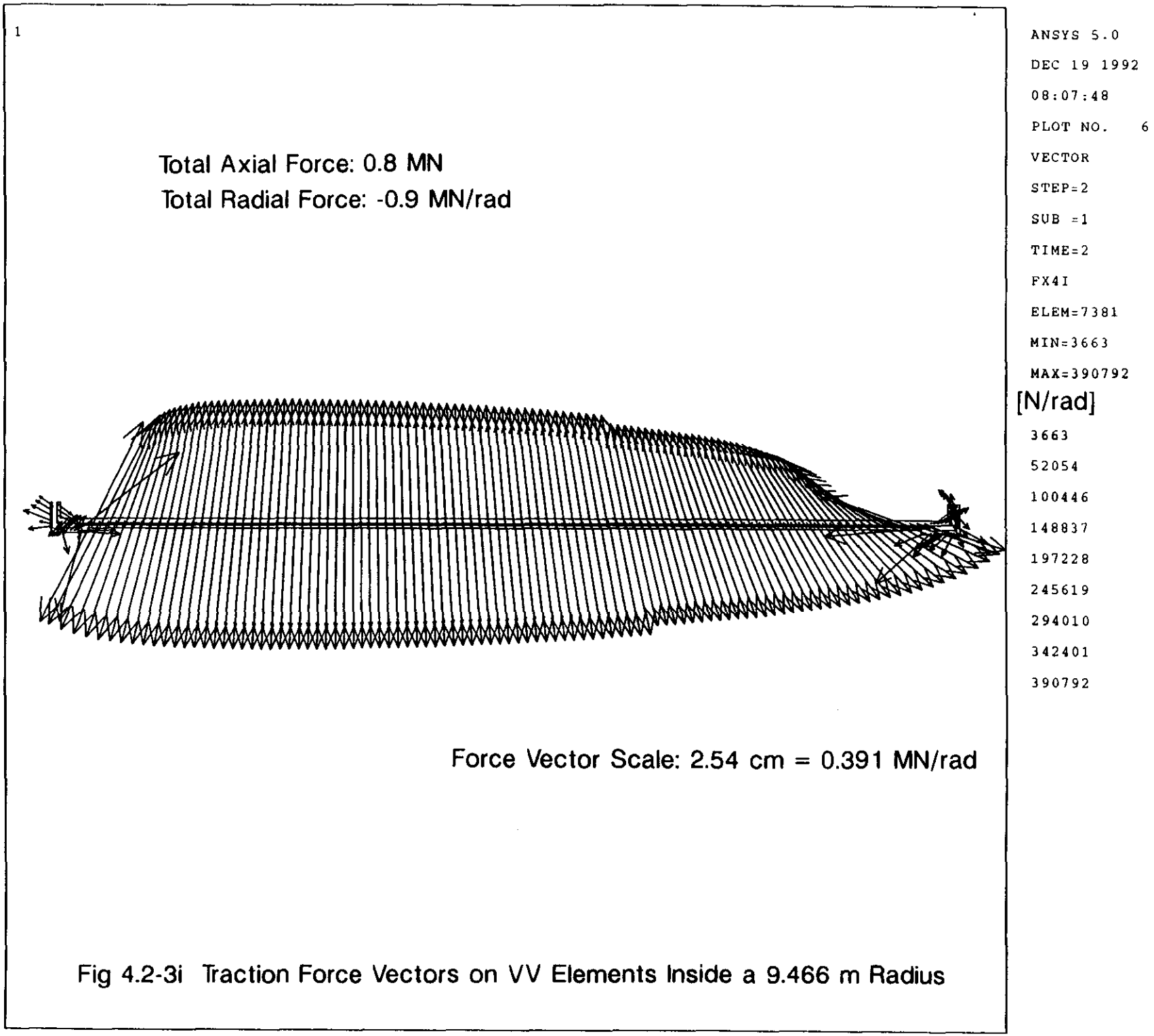

Fig 4.2-3i Traction Force Vectors on VV Elements Inside a 9.466 m Radius

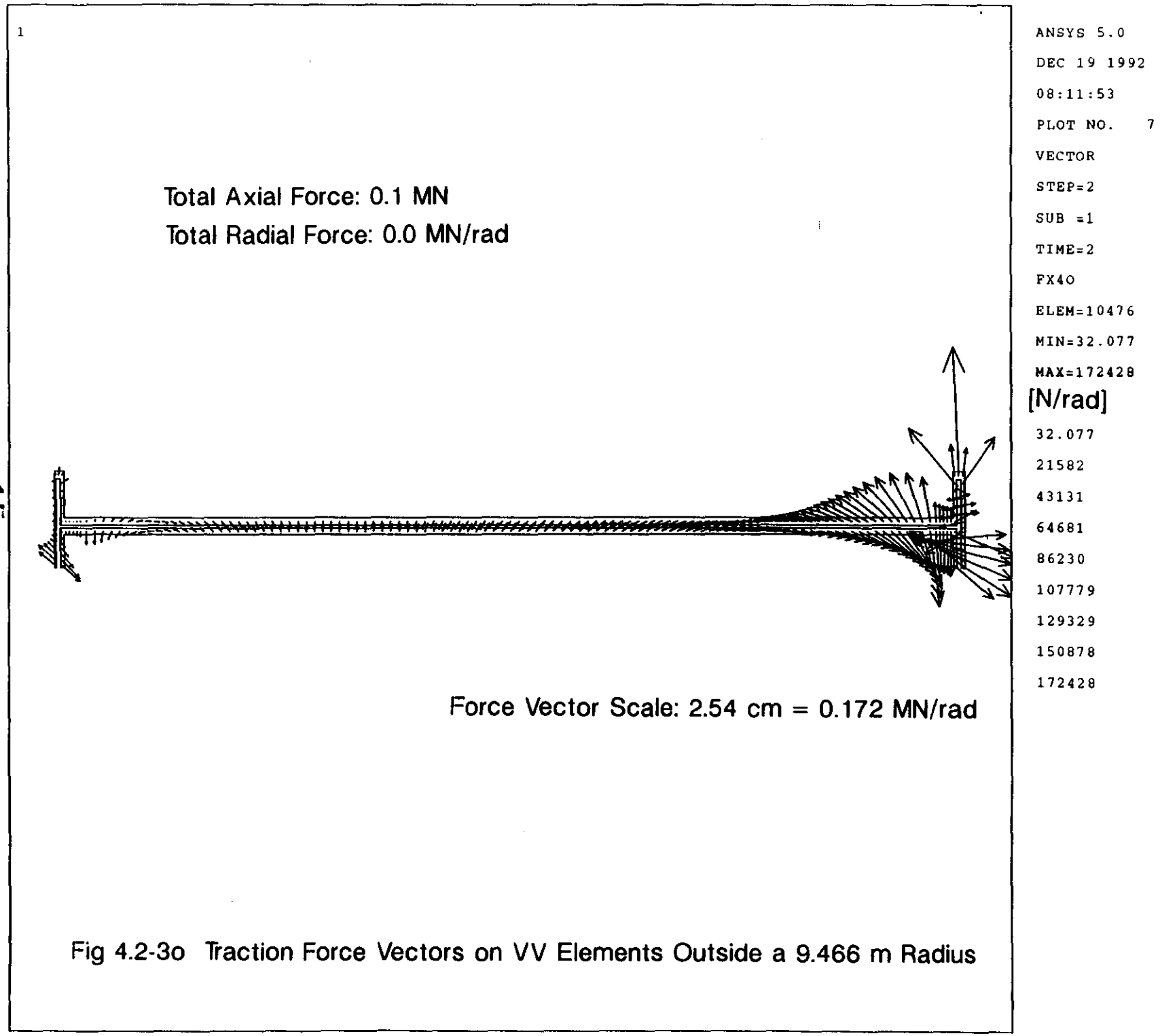

Fig 4.2-3o Traction Force Vectors on VV Elements Outside a 9.466 m Radius

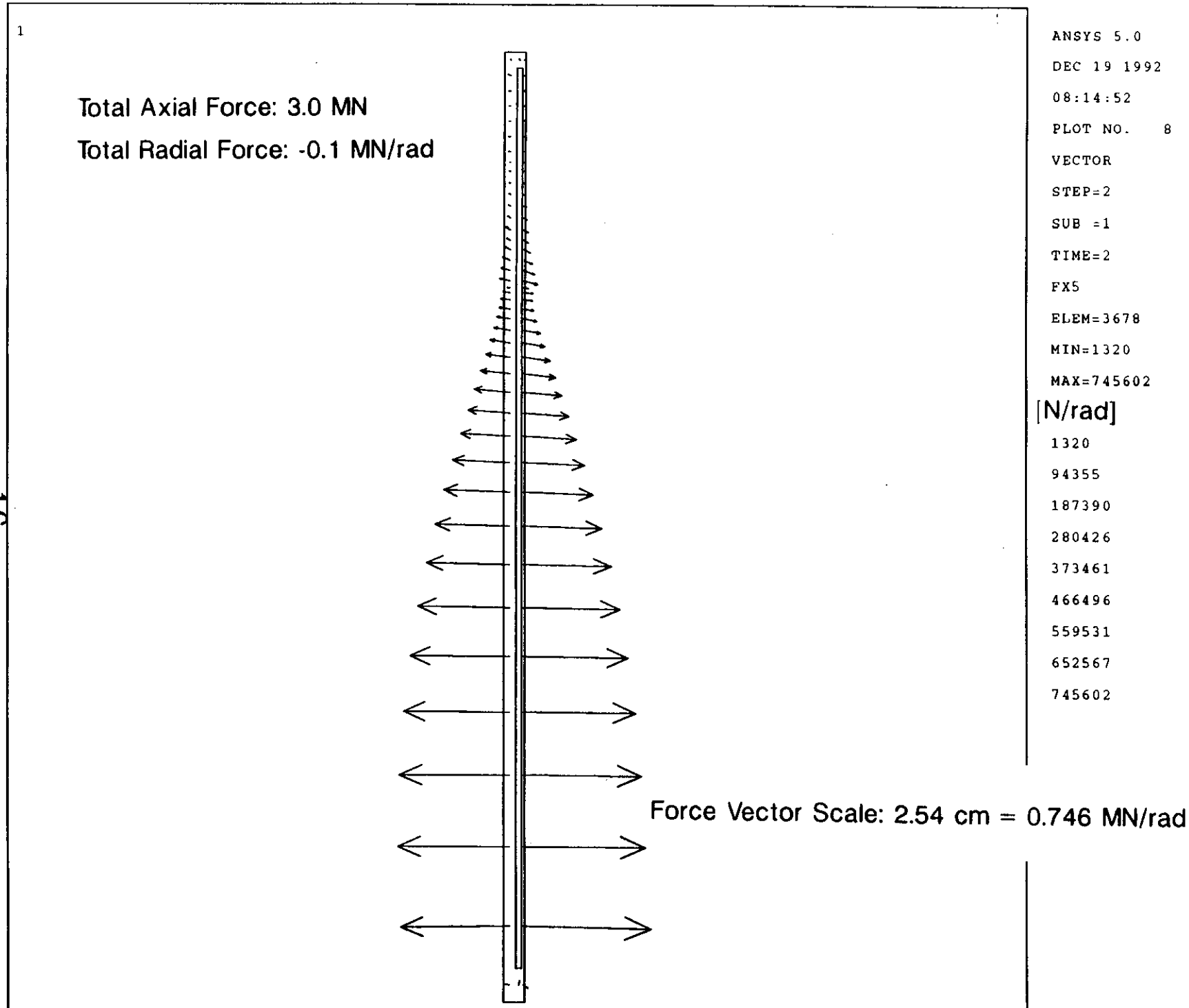

Fig 4.2-4 Traction Force Vectors on Central Membrane

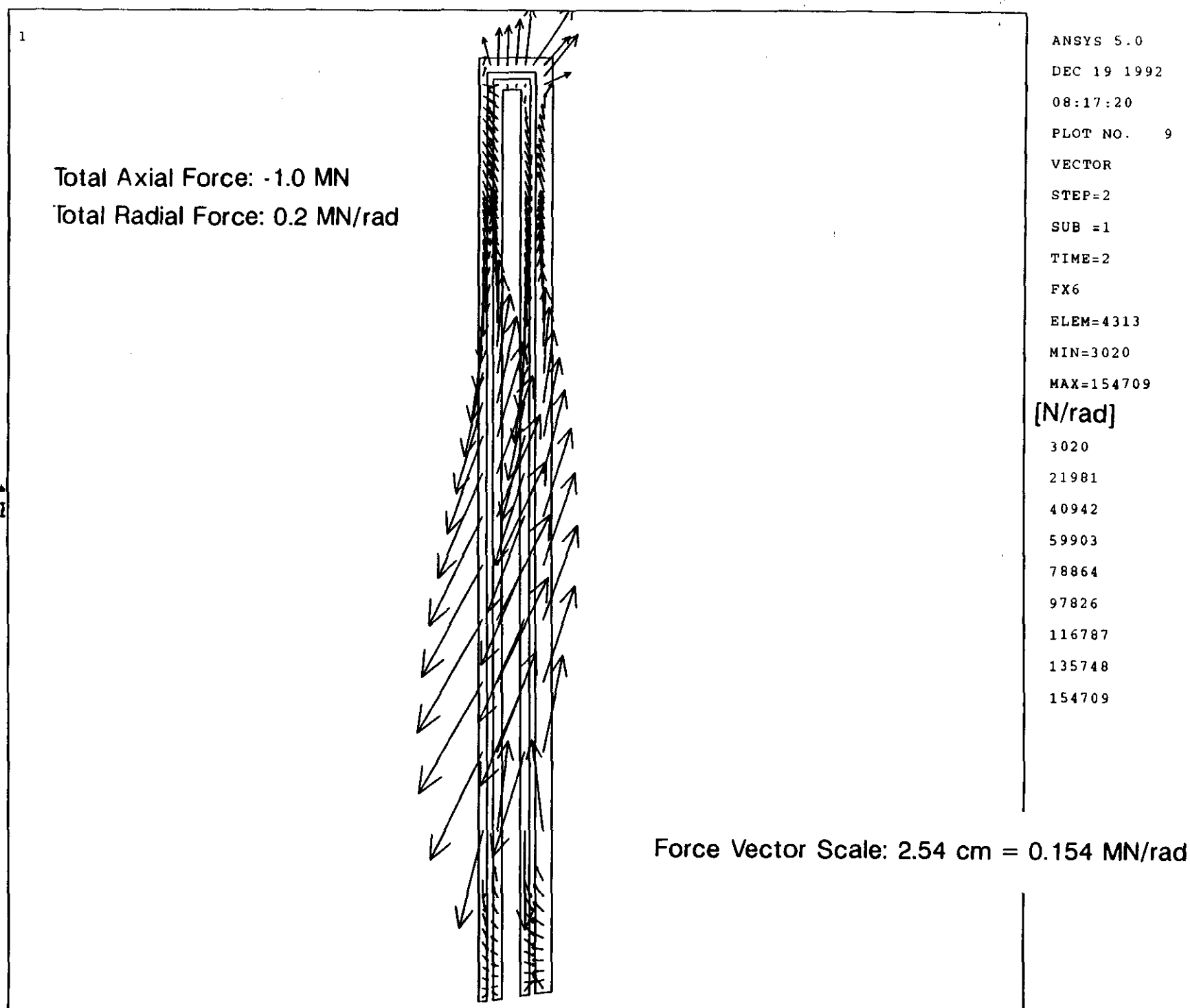

Fig 4.2-5 Traction Force Vectors on Flux Shaper Membranes